Research Article | Vol. 25, No. 26 | 25 Dec 2017 | OPTICS EXPRESS 32618

Optics EXPRESS

Accuracy analysis and improvement of visible light positioning based on VLC system using orthogonal frequency division multiple access

YITONG XU,[1] ZIXIONG WANG,[1,*] PEIXI LIU,[1] JIAN CHEN,[2] SHIYING HAN,[3] CHANGYUAN YU,[4] AND JINLONG YU[1]

[1] *School of Electrical and Information Engineering, Tianjin University, Tianjin 300072, China*
[2] *School of Telecommunications and Information Engineering, Nanjing University of Posts and Telecommunications, Nanjing 210003, China*
[3] *College of Electronic Information and Optical Engineering, Nankai University, Tianjin 300350, China*
[4] *Department of Electronic and Information Engineering, The Hong Kong Polytechnic University, Hong Kong, China*
[*] *wangzixiong@tju.edu.cn*

Abstract: In this paper, we proposed a system that realized simultaneously visible light positioning (VLP) and visible light communications (VLC) in the same band by using orthogonal frequency division multiple access (OFDMA). This system used the power of data sequence as the metric to estimate the transmission distances and consequently the receiver's position, without deteriorating the VLC's throughput. We theoretically analyzed the positioning errors in both overdetermined and determined VLP systems. In overdetermined VLP system, optimal selection of master light-emitting diode (LED) avoided the fluctuation of positioning error. Excluding the LED with longest transmission distance changed the overdetermined VLP system to determined VLP system, and reduced the positioning error. The power allocation scheme reduced further the positioning error in determined VLP system. This method was fast and effective. The well-matched theoretical and Monte-Carlo (MC) simulation results validated our proposed VLP based on VLC system using OFDMA.

OCIS codes: (060.2605) Free-space optical communication; (230.3670) Light-emitting diodes.

References and links

1. T. Komine and M. Nakagawa, "Fundamental analysis for visible-light communication system using LED lights," IEEE Trans. Consum. Electron. **50**, 100–107 (2004).
2. J. Armstrong, Y. A. Sekercioglu, and A. Neild, "Visible light positioning: a roadmap for international standardization," IEEE Commun. Mag. **51**, 68–73 (2013).
3. M. F. Keskin and S. Gezici, "Comparative theoretical analysis of distance estimation in visible light positioning systems," J. Lightw. Technol. **34**, 854–865 (2016).
4. M. Yasir, S. W. Ho, and B. N. Vellambi, "Indoor position tracking using multiple optical receivers," J. Lightw. Technol. **34**, 1166–1176 (2016).
5. M. Yasir, S. W. Ho, and B. N. Vellambi, "Indoor localization using visible light and accelerometer," in "IEEE Global Communications Conference (GLOBECOM)," (2013), pp. 3341–3346.
6. Z. Li, L. Feng, and A. Yang, "Fusion based on visible light positioning and inertial navigation using extended Kalman filters," Sensors **17**, 1093 (2017).
7. S. Y. Jung, S. Hann, and C. S. Park, "TDOA-based optical wireless indoor localization using LED ceiling lamps," IEEE Trans. Consum. Electron. **57**, 1592–1597 (2011).
8. T.-H. Do and M. Yoo, "An in-depth survey of visible light communication based positioning systems," Sensors **16**, E678 (2016).
9. T. Q. Wang, Y. A. Sekercioglu, A. Neild, and J. Armstrong, "Position accuracy of time-of-arrival based ranging using visible light with application in indoor localization systems," J. Lightwave Technol. **31**, 3302–3308 (2013).
10. T. Tanaka and S. Haruyama, "New position detection method using image sensor and visible light leds," in *Second International Conference on Machine Vision* (2009), pp. 150–153.
11. W. Gu, M. Aminikashani, P. Deng, and M. Kavehrad, "Impact of multipath reflections on the performance of indoor visible light positioning systems," J. Lightwave Technol. **34**, 2578–2587 (2016).

#313489 https://doi.org/10.1364/OE.25.032618
Journal © 2017 Received 27 Nov 2017; accepted 30 Nov 2017; published 14 Dec 2017

12. B. Lin, X. Tang, Z. Ghassemlooy, C. Lin, and Y. Li, "Experimental demonstration of an indoor VLC positioning system based on OFDMA," IEEE Photonics J. **9**, 1–9 (2017).
13. B. Lin, X. Tang, Z. Ghassemlooy, Y. Li, and S. Zhang, "An indoor VLC positioning system based on OFDMA," in *Asia Communications and Photonics Conference* (2016), p. AS1B.5.
14. G. Cossu, A. M. Khalid, P. Choudhury, R. Corsini, and E. Ciaramella, "3.4 Gbit/s visible optical wireless transmission based on RGB LED," Opt. Express **20**, B501–B506 (2012).
15. Y. Xu, Z. Wang, J. Chen, S. Han, C. Yu, and J. Yu, "Incorporate visible light communication into visible light positioning using orthogonal frequency division multiple access," in *Asia Communications and Photonics Conference* (2017), pp. M3F.4.
16. J. M. Kahn and J. R. Barry, "Wireless infrared communications," Proc. IEEE **85**, 265–298 (1997).
17. J. Armstrong, "OFDM for optical communications," J. Lightwave Technol. **27**, 189–204 (2009).
18. M. Aminikashani, W. Gu, and M. Kavehrad, "Indoor positioning with OFDM visible light communications," in *13th IEEE Annual Consumer Communications Networking Conference (CCNC)* (2016), pp. 505–510.
19. H. Marshoud, V. M. Kapinas, G. K. Karagiannidis, and S. Muhaidat, "Non-orthogonal multiple access for visible light communications," IEEE Photonics Technol. Lett. **28**, 51–54 (2016).
20. A. Burton, E. Bentley, H. L. Minh, Z. Ghassemlooy, N. Aslam, and S. K. Liaw, "Experimental demonstration of a 10BASE-T Ethernet visible light communications system using white phosphor light-emitting diodes," IET Circuits, Devices Systems **8**, 322–330 (2014).

1. Introduction

Light-emitting diode (LED) is an attractive illumination device for its long lifetime, low energy consumption, and low heat generation [1]. Since LED is a kind of current-driving device, when the high data rate modulation signal is added to the direct current (DC) of LED, both communication and illumination can be achieved simultaneously, without causing any flicker [2]. Besides visible light communications (VLC), indoor positioning is another gift brought by LED. The accuracy of visible light positioning (VLP) is on the order of centimeter, which is much better than global positioning system (GPS) and other radio frequency (RF) counterparts [3, 4]. Hence, VLP is a great candidate for indoor positioning, tracking and navigation [4–6].

In VLP system, triangulation is a widely used positioning technology, including time of arrival (TOA), time difference of arrival (TDOA), angle of arrival (AOA), and received signal strength (RSS) [7, 8]. In [9], Wang *et al* analyzed the Cramér-Rao bound (CRB) of positioning accuracy in the TOA technique. However, perfect synchronization between transmitter and receiver is a prerequisite. In the TDOA technique, the LEDs transmit information simultaneously [7]. However, a local oscillator is required to recover the signal, which increases the complexity of VLP. In the AOA technique, both the image sensor and acceleration sensor are used to distinguish the received signals from light sources with different colors [10]. Therefore, it is not suitable for illumination. The positioning accuracy based on RSS technique has also been investigated in the literature. In [11], Wu *et al* proposed a scheme to improve the accuracy of VLP by excluding the LED with low RSS. However, the theoretical analysis of positioning accuracy is absent. Lin *et al* demonstrated the feasibility of VLP using orthogonal frequency division multiple access (OFDMA) [12, 13]. Nevertheless, all the subcarriers are exclusively assigned between VLP and VLC in these works. Specifically, only three tones are selected for localization, and the rest subcarriers are used for communication. Therefore, the VLC throughput is degraded by using this scheme, when introducing VLP in the same system.

In this paper, we propose a system that realizes VLP and VLC simultaneously in the same band using OFDMA. In such a system, each LED occupies particular subcarrier blocks of the whole spectrum. The receiver position in terms of transmission distances is estimated by measuring the channel gain of each subcarrier block. The advantages of this VLP system are two-fold. Firstly, fewer orthogonal frequency division multiplexing (OFDM) frames are required to obtain the stable estimated position, since all the subcarriers are involved in positioning. Secondly, the positioning is achieved by using arbitrary modulation format, such as M-ary quadrature amplitude modulation (M-QAM) OFDM, which is widely used in VLC system to boost the throughput [14]. We study the positioning error in this VLP system using OFDMA, and find

Research Article | Vol. 25, No. 26 | 25 Dec 2017 | OPTICS EXPRESS 32620

that the critical factors in positioning error are the differences among the errors of square of estimated transmission distances. The positioning error is investigated in both overdetermined and determined VLP systems. In overdetermined VLP system, the positioning error fluctuates when different LEDs are selected as the master LED. The fluctuation of positioning error is cancelled by optimally selecting the master LED. The overdetermined VLP system is changed to determined VLP system by excluding the LED with longest transmission distance. In this case, the positioning error of the determined VLP system is smaller than that of the overdetermined VLP system. The positioning error of determined VLP system is reduced further by using power allocation scheme. The power allocation coefficients are obtained according to the estimated channel gains. This method is fast and effective. The well-matched theoretical and Monte-Carlo (MC) simulation results validate the VLP based on VLC system using OFDMA. Part of this work has been presented in [15].

The rest of the paper is organized as follows. Section 2 describes the VLP based on VLC system using OFDMA. Section 3 analyzes the positioning errors in overdetermined VLP system, determined VLP system and determined VLP system using power allocation scheme. Finally, the concluding remarks are summarized in Section 4.

2. VLP based on VLC system using OFDMA

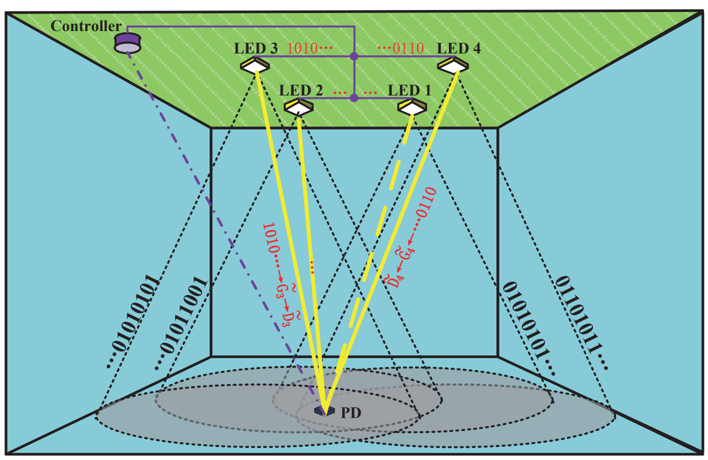

Fig. 1. Simultaneous realization of VLP and VLC using OFDMA.

Fig. 1 shows the diagram of the system that realizes VLP and VLC simultaneously in the same band using OFDMA. In this system, the whole bandwidth is divided to subcarrier blocks. The particular subcarrier blocks are exclusively assigned to the corresponding LEDs. The LEDs transmit different data sequences to the photo-detector (PD) for VLC. The VLC's receiver measures the power of particular data sequences to estimate the channel gains and consequently the transmission distances. Based on the estimated transmission distances and the LEDs' locations, the VLP is realized without degrading the VLC's throughput. In this section, firstly we introduce the VLC system model using M-QAM OFDM. After that, we describe the system that realizes VLP and VLC simultaneously in the same band in detail.

2.1. VLC model

Both VLC and VLP use LED as the light source. The LED is a current-driving device. It is driven by the DC I_0 and alternating current (AC) $i(t)$ components for illumination and communication, respectively. We use M-QAM OFDM signal as the AC driving component $i(t)$. The magnitude of $i(t)$ is confined by the modulation index (MI), which is defined as the ratio of maximum absolute value of $i(t)$ to I_0, *i.e.*, MI = $\frac{\max|i(t)|}{I_0}$. It is assumed that the LED works in the linear region, *i.e.*, the LED's driving signal is proportional to their output power. Let K denote the ratio of LED instantaneous power to the driving signal. The LED's output power is

$$P_{\mathrm{T}}(t) = K[I_0 + i(t)] = P_0 + Ki(t), \quad (1)$$

where $P_0 = KI_0$ is the LED's DC output power and $Ki(t)$ is the LED's AC output power.

The modulated LED output light propagates through indoor VLC channel. If we do not consider the light reflections, the VLC channel gain is defined as [1]

$$G = \frac{(m+1)A}{2\pi D^2}\cos^m(\phi)\cos(\psi), \quad (2)$$

where A is the PD's area, D is the transmission distance between LED and PD, ϕ is the angle of radiation, and ψ is the angle of incidence. The order of Lambertian radiation pattern is $m = -\ln 2/\ln(\cos\Phi_{1/2})$, where $\Phi_{1/2}$ is the transmitter's semiangle at half power [16]. Let h denote the vertical distance between the LED and PD. Hence, $\cos(\psi) = \cos(\phi) = \frac{h}{D}$. The channel gain in Eq. (2) becomes

$$G = \frac{(m+1)Ah^{m+1}}{2\pi}\frac{1}{D^{m+3}}. \quad (3)$$

The received optical signal is $P_{\mathrm{R}}(t) = RGP_{\mathrm{T}}(t) = RGP_0 + RGKi(t)$, where R is the responsivity of PD. The DC component RGP_0 is removed by the DC block after photo-detection. Therefore, the converted electrical signal is given by

$$y(t) = s(t) + n(t) = RG\delta(t-\tau) * Ki(t) + n(t). \quad (4)$$

$s(t) = RG\delta(t-\tau) * Ki(t)$ is the recovered information signal, where $*$ represents convolution and τ is the propagation delay. $n(t)$ is the additive white Gaussian noise (AWGN). After passing through the fast Fourier transform (FFT) module, the recovered data is given by

$$Y(f) = S(f) + N(f) = RGKI(f)\exp(-j2\pi f\tau) + N(f). \quad (5)$$

The communication performance in terms of bit error rate (BER) is evaluated by comparing the detected data and original data. The VLC system using OFDM is shown in Fig. 2. Note that cyclic prefix (CP) module is not shown Fig. 2, since the light reflections are not considered.

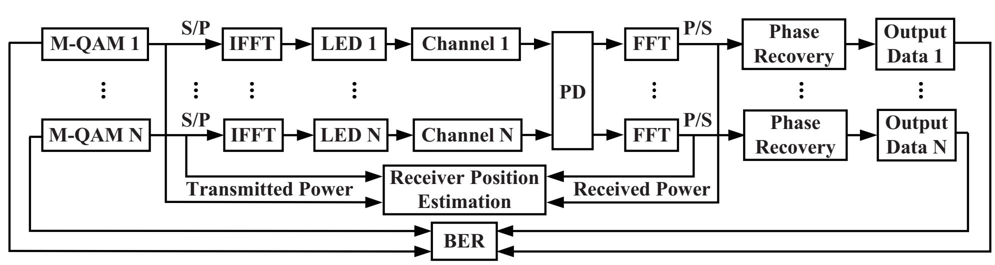

Fig. 2. The system that realizes VLC and VLP simultaneously in the same band.

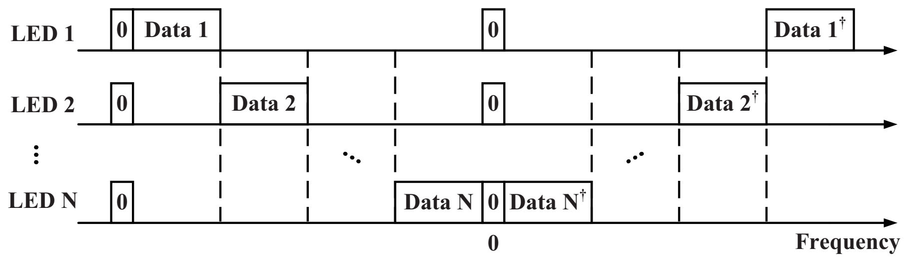

Fig. 3. Spectrum allocation of VLP system using OFDMA. †: Hermitian symmetry.

2.2. *VLP and VLC system using OFDMA*

In this subsection, we realize VLP in the existing VLC system as described in Section 2.1. The system is shown in Figs. 1 and 2, where VLC and VLP are realized simultaneously in the same band using OFDMA. Suppose that there are N LEDs mounted in the ceiling. As shown in Fig. 3, the whole bandwidth is divided into $2N$ subcarrier blocks. Each LED occupies two subcarrier blocks. The data allocated to DC term and Nyquist term are zeros [17], since Hermitian symmetry is used to guarantee the real output of OFDM signal. The controller in Fig. 1 assigns the data to different subcarrier blocks, and lets the OFDM signals at the output of inverse fast Fourier transform (IFFT) modules to drive the corresponding LEDs. The LEDs emit the modulated light, which is collected by the receiver. The receiver converts the light into one electrical signal, and analyzes the signal's power in each subcarrier block to estimate the channel gain. The channel gain is estimated by comparing the power of received signal with the power of transmitted signal, which is given by

$$\tilde{G} = \left\{ \frac{\mathbb{E}\left[|Y(f)|^2\right]}{R^2K^2\mathbb{E}\left[|I(f)|^2\right]} \right\}^{\frac{1}{2}} = \left\{ \frac{R^2G^2K^2\mathbb{E}\left[|I(f)|^2\right] + \mathbb{E}\left[|N(f)|^2\right]}{R^2K^2\mathbb{E}\left[|I(f)|^2\right]} \right\}^{\frac{1}{2}}, \tag{6}$$

where the intermediate item $2\mathbb{E}\left[\Re\left\{S(f)N^*(f)\right\}\right]$ in the numerator vanishes. This method to estimate channel gain is suitable for arbitrary modulation format in VLC system.

According to Eqs. (3) and (6), the transmission distance is estimated. The estimated transmission distances and the LEDs' locations are necessary to estimate the receiver's position. Therefore, the critical issue in VLP using OFDMA is how to obtain the LED's location from the power of each subcarrier block. We use pulse position modulation (PPM) code to distinguish LEDs. The frame structure is shown in Fig. 4. The first frame uses PPM code, while the rest frames do not. More specifically, each LED is assigned an identification (ID) number in the first frame, where the ID number's length is not longer than half of the subcarrier block's length. The ID represents the LED's location. When the LED's ID is '0', the PPM code is '01', *i.e.*, the data is allocated to the second subcarrier. Otherwise, the PPM code is '10', *i.e.*, the data is allocated to the first subcarrier. By using PPM, the data is allocated to only one of the two adjacent subcarriers. The LED's ID is decoded by comparing the power of adjacent subcarriers in each subcarrier block. Therefore, the LED's location is obtained.

In the rest frames, the data is allocated to all the available subcarriers for both VLP and VLC, if the assignment of LEDs for VLP is not changed. The transmission distances in terms of channel gains are obtained by evaluating the average received power of the data in each subcarrier and comparing it with the transmitted power. Consequently, the receiver's location is estimated by using the LEDs' locations and estimated transmission distances.

Optics EXPRESS

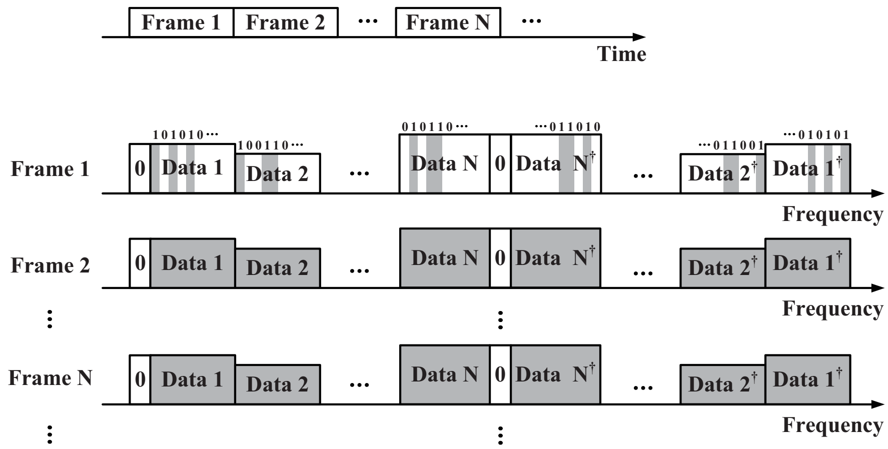

Fig. 4. Frame structure for VLP system using OFDMA. †: Hermitian symmetry. Dark: subcarriers allocated by data.

3. Accuracy analysis of VLP using OFDMA

In this section, we analyze the positioning accuracy of VLP system using OFDMA, based on the LEDs' locations and estimated transmission distances. According to Fig. 2, there are N LEDs mounted in the ceiling. Their locations are denoted as $\left[X_i, Y_i, Z_i\right]^{\mathrm{T}}, i \in \mathbb{L} = \{1, 2, \ldots, N\}$. Let $\left[\tilde{X}, \tilde{Y}, \tilde{Z}\right]^{\mathrm{T}}$ denote the receiver's estimated location. Using the geometry property, we have

$$\left\|\left[\tilde{X}, \tilde{Y}, \tilde{Z}\right] - \left[X_i, Y_i, Z_i\right]\right\|_2^2 = \tilde{D}_i^2, \qquad i \in \mathbb{L}, \tag{7}$$

where $\tilde{D}_i$ are the estimated transmission distances. Suppose that the height of receiver is known. The two-dimensional positioning is obtained by letting one equation subtract other equations in Eq. (7), which has the following form

$$\mathbf{A}\tilde{\boldsymbol{p}} = \tilde{\boldsymbol{b}}. \tag{8}$$

The items in Eq. (8) are

$$\mathbf{A} = 2\begin{bmatrix} X_{\mathrm{S}_1} - X_{\mathrm{M}} & Y_{\mathrm{S}_1} - Y_{\mathrm{M}} \\ X_{\mathrm{S}_2} - X_{\mathrm{M}} & Y_{\mathrm{S}_2} - Y_{\mathrm{M}} \\ \vdots & \vdots \\ X_{\mathrm{S}_{N-1}} - X_{\mathrm{M}} & Y_{\mathrm{S}_{N-1}} - Y_{\mathrm{M}} \end{bmatrix}, \tag{9}$$

$$\tilde{\boldsymbol{p}} = \begin{bmatrix} \tilde{X} \\ \tilde{Y} \end{bmatrix} = \begin{bmatrix} X \\ Y \end{bmatrix} + \begin{bmatrix} \Delta X \\ \Delta Y \end{bmatrix}, \tag{10}$$

and

$$\tilde{\boldsymbol{b}} = \begin{bmatrix} X_{\mathrm{S}_1}^2 - X_{\mathrm{M}}^2 + Y_{\mathrm{S}_1}^2 - Y_{\mathrm{M}}^2 + \tilde{D}_{\mathrm{M}}^2 - \tilde{D}_{\mathrm{S}_1}^2 \\ X_{\mathrm{S}_2}^2 - X_{\mathrm{M}}^2 + Y_{\mathrm{S}_2}^2 - Y_{\mathrm{M}}^2 + \tilde{D}_{\mathrm{M}}^2 - \tilde{D}_{\mathrm{S}_2}^2 \\ \vdots \\ X_{\mathrm{S}_{N-1}}^2 - X_{\mathrm{M}}^2 + Y_{\mathrm{S}_{N-1}}^2 - Y_{\mathrm{M}}^2 + \tilde{D}_{\mathrm{M}}^2 - \tilde{D}_{\mathrm{S}_{N-1}}^2 \end{bmatrix}. \tag{11}$$

In Eq. (9), we name the LED as the master LED, whose coordinate is $\left[X_{\mathrm{M}}, Y_{\mathrm{M}}\right]^{\mathrm{T}}$. The master LED corresponds to the equation that subtracts other equations in Eq. (7). The remainder LEDs are named as the slave LEDs, whose coordinates are $\left[X_{\mathrm{S}_j}, Y_{\mathrm{S}_j}\right]^{\mathrm{T}}, j = 1, 2, \ldots, N-1$. Thus,

$\mathrm{M}, \mathrm{S}_j \in \mathbb{L}, \mathrm{M} \neq \mathrm{S}_j$. Let $\boldsymbol{p} = [X, Y]^{\mathrm{T}}$ and $\Delta\boldsymbol{p} = [\Delta X, \Delta Y]^{\mathrm{T}}$ denote the receiver's actual position and the positioning error, respectively. Eq. (8) are recast as

$$\mathbf{A}(\boldsymbol{p} + \Delta\boldsymbol{p}) = \boldsymbol{b} + \Delta\boldsymbol{b}, \tag{12}$$

where

$$\boldsymbol{b} = \begin{bmatrix} X_{\mathrm{S}_1}^2 - X_{\mathrm{M}}^2 + Y_{\mathrm{S}_1}^2 - Y_{\mathrm{M}}^2 + D_{\mathrm{M}}^2 - D_{\mathrm{S}_1}^2 \\ X_{\mathrm{S}_2}^2 - X_{\mathrm{M}}^2 + Y_{\mathrm{S}_2}^2 - Y_{\mathrm{M}}^2 + D_{\mathrm{M}}^2 - D_{\mathrm{S}_2}^2 \\ \vdots \\ X_{\mathrm{S}_{N-1}}^2 - X_{\mathrm{M}}^2 + Y_{\mathrm{S}_{N-1}}^2 - Y_{\mathrm{M}}^2 + D_{\mathrm{M}}^2 - D_{\mathrm{S}_{N-1}}^2 \end{bmatrix}, \quad \Delta\boldsymbol{b} = \begin{bmatrix} \Delta D_{\mathrm{M}}^2 - \Delta D_{\mathrm{S}_1}^2 \\ \Delta D_{\mathrm{M}}^2 - \Delta D_{\mathrm{S}_2}^2 \\ \vdots \\ \Delta D_{\mathrm{M}}^2 - \Delta D_{\mathrm{S}_{N-1}}^2 \end{bmatrix}.$$

By using least squares estimation (LSE) method [18] to solve Eq. (12), we can obtain the positioning error vector $\Delta\boldsymbol{p}$ as

$$\Delta\boldsymbol{p} = \begin{bmatrix} \Delta X \\ \Delta Y \end{bmatrix} = \left(\mathbf{A}^{\mathrm{T}}\mathbf{A}\right)^{-1}\mathbf{A}^{\mathrm{T}}\Delta\boldsymbol{b}. \tag{13}$$

The positioning error $\|\Delta\boldsymbol{p}\|_2$ is the 2-norm of the positioning error vector $\Delta\boldsymbol{p}$. Eq. (13) indicates that the differences between ΔD_{M}^2 and $\Delta D_{\mathrm{S}j}^2$ are critical to the positioning error. Choosing different LEDs as the master LED leads to different positioning errors.

According to Eqs. (3) and (6), the square of estimated transmission distance for the ith LED, $\forall i \in \mathbb{L}$ is

$$\tilde{D}_i^2 = \left\{ \frac{1}{D_i^{2(m+3)}} + \frac{\sigma_{\mathrm{N}}^2}{\left[\frac{RK(m+1)Ah^{m+1}}{2\pi}\right]^2 \mathbb{E}\left[|I(f)|^2\right]} \right\}^{-\frac{1}{m+3}}, \tag{14}$$

where $\sigma_{\mathrm{N}}^2 = \mathbb{E}\left[|N(f)|^2\right]$ is the noise power. The error of square of estimated transmission distance ΔD_i^2 is defined as,

$$\Delta D_i^2 = \tilde{D}_i^2 - D_i^2 = \left\{ \frac{1}{D_i^{2(m+3)}} + \frac{\sigma_{\mathrm{N}}^2}{\left[\frac{RK(m+1)Ah^{m+1}}{2\pi}\right]^2 \mathbb{E}\left[|I(f)|^2\right]} \right\}^{-\frac{1}{m+3}} - D_i^2. \tag{15}$$

In the rest of this paper, we will study the positioning error $\|\Delta\boldsymbol{p}\|_2$ in terms of ΔD_i^2 by both theoretical analysis and MC simulation. Note that the MC simulation results are averaged, according to Eq. (6).

3.1. Simulation setup

The simulation is carried out in a spacious room (16 m × 16 m × 5 m). The positioning error performance is studied in the space of 8 m × 8 m × 5 m, which is the inner frame as shown in Fig. 5. Since the receiver is quite far from the walls, we do not consider the reflection effect on positioning error. We assume that there are four identical LEDs mounted in the ceiling, where the LEDs are distributed evenly. The four LEDs' locations are $[2\text{ m}, 2\text{ m}, 5\text{ m}]^{\mathrm{T}}$, $[-2\text{ m}, 2\text{ m}, 5\text{ m}]^{\mathrm{T}}$, $[-2\text{ m}, -2\text{ m}, 5\text{ m}]^{\mathrm{T}}$ and $[2\text{ m}, -2\text{ m}, 5\text{ m}]^{\mathrm{T}}$, respectively. The receiver is parallel to all the LEDs. The LED's semiangle at half power is 60°, which means that the order of Lambertian radiation pattern $m = 1$. The MI is no larger than 0.6. The responsivity of PD is $R = 0.6$ A/W. The LED launching power is 3 W and the total bandwidth B_d is 10 MHz, if not explicitly stated.

Optics EXPRESS

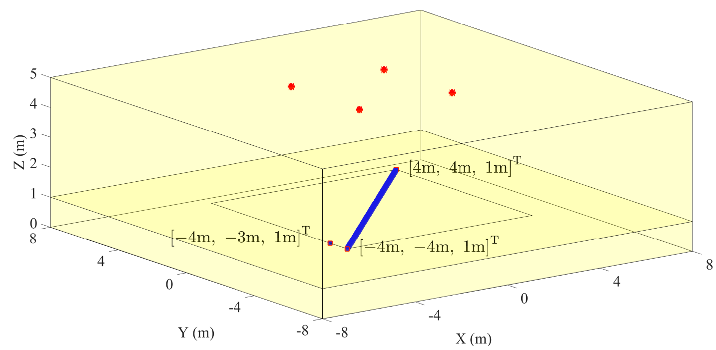

Fig. 5. Locations of LEDs and receivers. Red: LEDs, blue: receivers, inner frame: receiver region.

3.2. Positioning error in overdetermined VLP system

The VLP system is overdetermined when all the four LEDs ($N = 4$) are used for positioning, as described in Eq. (13). The positioning error is mainly determined by the items in Δb, *i.e.*, the differences between ΔD_{M}^2 and $\Delta D_{\mathrm{S}_j}^2, j = 1, 2, 3$. In this subsection, we study the performances of ΔD_{M}^2 and $\Delta D_{\mathrm{M}}^2 - \Delta D_{\mathrm{S}_j}^2$, $\forall \mathrm{M}, \mathrm{S}_j \in \mathbb{L}, \mathrm{M} \neq \mathrm{S}_j$. The receiver locates at $[-4\ \mathrm{m}, -3\ \mathrm{m}, 1\ \mathrm{m}]^{\mathrm{T}}$, as shown in Fig. 5. The transmission distances between the four LEDs and the receiver are 8.78 m, 6.71 m, 4.58 m and 7.28 m, respectively. The performance of $\Delta D_i^2, i \in \mathbb{L}$, under these transmission distances are shown in Fig. 6(a). All ΔD_i^2 are negative. ΔD_i^2 becomes smaller as the transmission distance increases. The smallest ΔD_i^2 is ΔD_1^2 (-1.357 m^2), where LED 1 is with the longest transmission distance. The largest ΔD_i^2 is ΔD_3^2 (-0.002 m^2), where LED 3 is with the shortest transmission distance. The theoretical and MC simulations match very well, which validates Eq. (15).

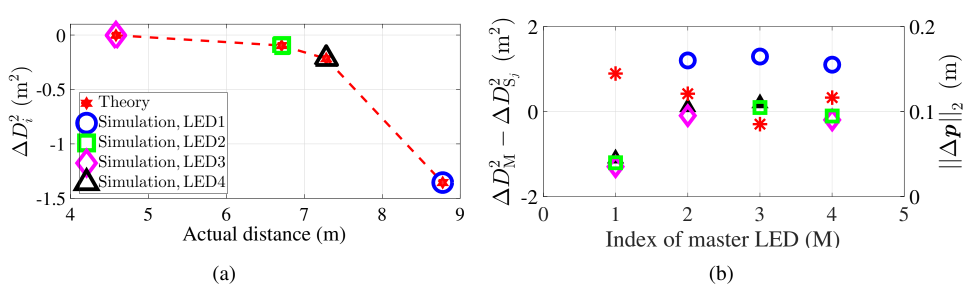

Fig. 6. (a) $\Delta D_i^2, i = 1, 2, 3, 4$, (b) $\Delta D_{\mathrm{M}}^2 - \Delta D_{\mathrm{S}_j}^2$ and $||\Delta \boldsymbol{p}||_2$, blue: slave LED 1, green: slave LED 2, pink: slave LED 3, black: slave LED 4, red: $||\Delta \boldsymbol{p}||_2$.

The performance of $\Delta D_{\mathrm{M}}^2 - \Delta D_{\mathrm{S}_j}^2$ and $||\Delta \boldsymbol{p}||_2$ are shown in Fig. 6(b). When LED 1 is selected as the master LED (M = 1), $\Delta D_{\mathrm{M}}^2 - \Delta D_2^2$, $\Delta D_{\mathrm{M}}^2 - \Delta D_3^2$ and $\Delta D_{\mathrm{M}}^2 - \Delta D_4^2$ are most distinct. In this case, the norm of $\Delta \boldsymbol{b}$ is 2.09 m^2 and the corresponding positioning error $||\Delta \boldsymbol{p}||_2$ is 0.145 m. When LEDs 2, 3, and 4 are selected as the master LED (M = 2, 3, 4), their positioning errors $||\Delta \boldsymbol{p}||_2$ are 0.121 m, 0.085 m, and 0.117 m, respectively. Therefore, the fluctuation of positioning error occurs in the overdetermined VLP system, and the positioning error is minimum when LED 3 is the master LED. We should select the LED with the shortest transmission distance as the master LED to avoid the fluctuation of positioning error.

This strategy is verified by investigating the positioning error at the room's diagonal, where the receiver locates from $[-4\text{ m}, -4\text{ m}, 1\text{ m}]^T$ to $[4\text{ m}, 4\text{ m}, 1\text{ m}]^T$, as shown in Fig. 5. The transmission distances follow $D_3 < D_2 = D_4 < D_1$, when the receiver's horizontal location is less than zero. The positioning error follows $||\Delta \boldsymbol{p}_3||_2 < ||\Delta \boldsymbol{p}_2||_2 = ||\Delta \boldsymbol{p}_4||_2 < ||\Delta \boldsymbol{p}_1||_2$, when the corresponding LED is selected as the master LED, as shown in Fig. 7. The trend of positioning error is inverse, when the receiver locates at the other half of the diagonal. We can see from Figs. 6 and 7 that, the longer transmission distance leads to the more distinct $\Delta D_M^2 - \Delta D_{S_1}^2$, $\Delta D_M^2 - \Delta D_{S_2}^2$ and $\Delta D_M^2 - \Delta D_{S_3}^2$, and thereafter leads to larger positioning error. Hence, we should select the LED with the shortest transmission distance as the master LED to avoid the positioning error fluctuation and to minimize the positioning error in overdetermined VLP system.

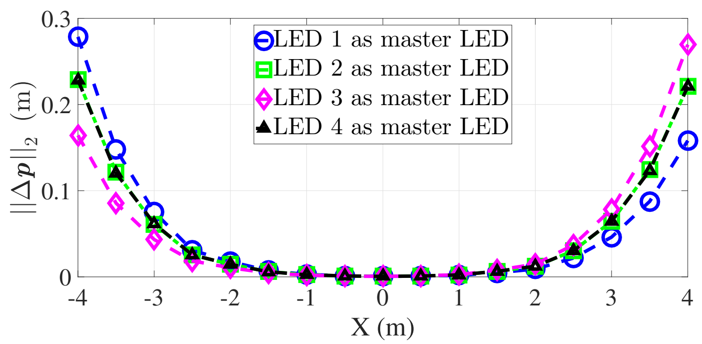

Fig. 7. Positioning error in overdetermined VLP system using OFDMA, when the receiver locates at the diagonal of the room.

3.3. *Positioning error in determined VLP system*

In Section 3.2, we analyzed the positioning error performance in overdetermined VLP system using OFDMA, because usually N (>3) LEDs are mounted in the ceiling for the convenience of illumination. However, three out of N LEDs are enough for two-dimensional VLP system. The overdetermined VLP system is consequently changed to determined VLP system. In this subsection, we study the positioning error in the determined VLP system using OFDMA.

As shown in Fig. 5, there are four LEDs mounted in the ceiling. We use only three of them for positioning, *i.e.*, excluding one LED in the VLP system using OFDMA. In this case, the whole band is occupied by three LEDs, *i.e.*, $N = 3$ in Fig. 4. The expression of positioning error vector $\Delta \boldsymbol{p}$ in Eq. (13) becomes

$$\Delta \boldsymbol{p} = \begin{bmatrix} \Delta X \\ \Delta Y \end{bmatrix} = \left(\mathbf{A}'^T \mathbf{A}'\right)^{-1} \mathbf{A}'^T \Delta \boldsymbol{b}', \tag{16}$$

where $\mathbf{A}' = 2\begin{bmatrix} X_{S_1} - X_M & Y_{S_1} - Y_M \\ X_{S_2} - X_M & Y_{S_2} - Y_M \end{bmatrix}$ and $\Delta \boldsymbol{b}' = \begin{bmatrix} \Delta D_M^2 - \Delta D_{S_1}^2 \\ \Delta D_M^2 - \Delta D_{S_2}^2 \end{bmatrix}$. Since the positioning system is determined, the selection of master LED does not affect the positioning error.

The positioning error and estimated position are shown in Fig. 8, when the receiver locates at $[-4\text{ m}, -3\text{ m}, 1\text{ m}]^T$. The positioning error is highly affected by the excluded LED. The positioning errors are 0.029 m, 0.145 m, 0.212 m, and 0.158 m, by excluding LEDs 1 to 4, respectively. The positioning error is 0.085 m in overdetermined VLP system, as described in Section 3.2. The positioning error is reduced, only by excluding LED 1 in the overdetermined VLP system. Since $D_1 > D_4 > D_2 > D_3$, we should excluding the LED with longest transmission distance to achieve the reduction of positioning error in determined VLP system.

The performance of positioning error in the determined VLP system using OFDMA is also studied in Fig. 9, where the receiver locates at the room's diagonal from $[-4\text{ m}, -4\text{ m}, 1\text{ m}]^T$ to

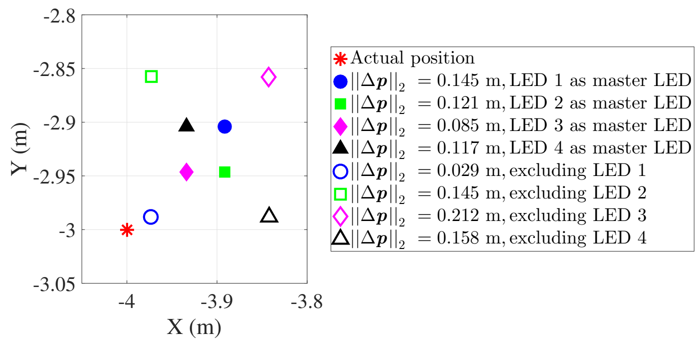

Fig. 8. Estimated position for the receiver at $[-4\text{ m}, -3\text{ m}, 1\text{ m}]^T$ in overdetermined (filled) and determined (hollow) VLP systems using OFDMA.

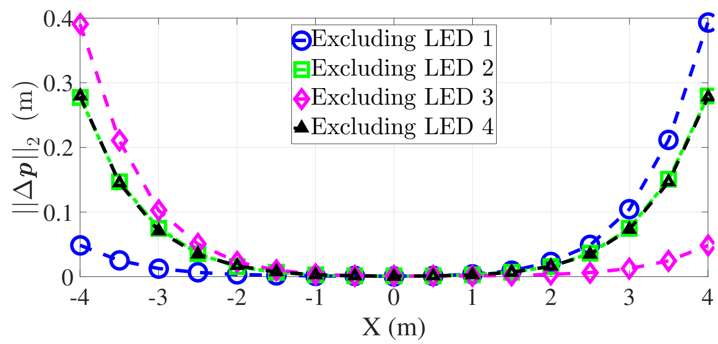

Fig. 9. Positioning error in determined VLP system using OFDMA for the receivers at the diagonal of the room.

$[4\text{ m}, 4\text{ m}, 1\text{ m}]^T$. The transmission distances follow $D_3 < D_2 = D_4 < D_1$, when the receiver's horizontal location is less than zero. The positioning error follows $||\Delta \boldsymbol{p}_1||_2 < ||\Delta \boldsymbol{p}_2||_2 = ||\Delta \boldsymbol{p}_4||_2 < ||\Delta \boldsymbol{p}_3||_2$, when the corresponding LED is excluded in the determined VLP system. Comparing Fig. 9 with Fig. 7, the positioning error is reduced only when the LED with largest transmission distance (LED 1) is excluded. For example, when the receiver locates at $[-4\text{ m}, -4\text{ m}, 1\text{ m}]^T$, the positioning errors in the overdetermined and determined VLP system using OFDMA are 0.164 m and 0.049 m, respectively. This determined VLP system brings 0.115 m improvement of positioning accuracy. However, the positioning errors are increased, when the rest LEDs are excluded in the determined VLP system. This trend of positioning error is inverse, when the receiver locates as the other half of the diagonal.

3.4. Positioning error in determined VLP system with power allocation

In this subsection, we propose a power allocation scheme to reduce the positioning error further in determined VLP system using OFDMA. According to Eq. (16), the positioning error is reduced if the items of $\Delta \boldsymbol{b}'$ is are decreased. The power allocation scheme allocates different power to the electrical modulation signal for each LED, which is shown in Fig. 10. The receiver calculates the power allocation coefficient $\alpha^2_{\text{PA},i,k}$ based on the estimated channel gain $\tilde{G}_{\text{PA},i,k}$ for the modulation signal of ith LED in kth positioning trial. The $\alpha^2_{\text{PA},i,k}$ are sent back to the controller to allocate the power for $(k+1)$th positioning trial via the uplink, as shown in Fig. 1. The uplink can be realized by either RF or infrared [19, 20]. The $\alpha^2_{\text{PA},i,k}$ is identical to the subcarriers in each subcarrier block. The overall power of electrical modulation signals using the power allocation scheme

Optics EXPRESS

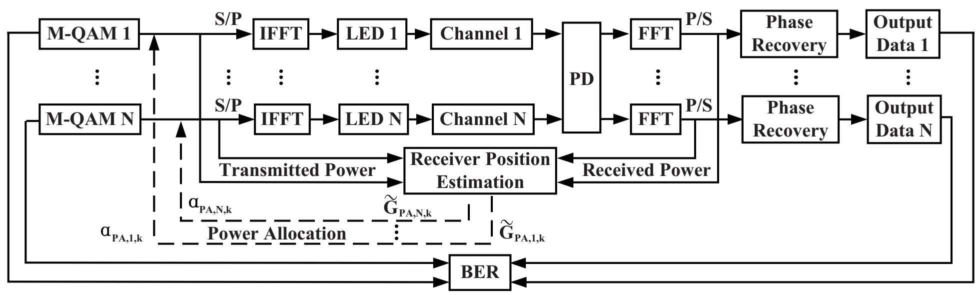

Fig. 10. VLP system using OFDMA and power allocation.

is the same as that without using power allocation scheme. What's more, the power of all the recovered electrical signals should be identical based on the estimation of channel gain $\tilde{G}_{\mathrm{PA},i,k}$.

Take the receiver at $[-4\text{ m}, -3\text{ m}, 1\text{ m}]^{\mathrm{T}}$ for example. As shown in Section 3.3, excluding LED 1 changes the overdetermined VLP system to determined VLP system. Hence, for each subcarrier block we have

$$\sum_{i=2}^{4} \alpha_{\mathrm{PA},i,k}^{2} = 3 \tag{17}$$

$$\alpha_{\mathrm{PA},2,k}^{2} \tilde{G}_{\mathrm{PA},2,k}^{2} = \alpha_{\mathrm{PA},3,k}^{2} \tilde{G}_{\mathrm{PA},3,k}^{2} = \alpha_{\mathrm{PA},4,k}^{2} \tilde{G}_{\mathrm{PA},4,k}^{2}. \tag{18}$$

By solving Eqs. (17) and (18), we have

$$\alpha_{\mathrm{PA},i,k}^{2} = \frac{\frac{3}{\tilde{G}_{\mathrm{PA},i,k}^{2}}}{\sum_{i=2}^{4} \frac{1}{\tilde{G}_{\mathrm{PA},i,k}^{2}}}, \qquad i = 2, 3, 4. \tag{19}$$

Using power allocation scheme, the frequency-domain received signal of the ith LED in Eq. (5) becomes

$$Y_{\mathrm{PA},i,k}(f) = S_{\mathrm{PA},i,k}(f) + N(f) = RG_i K \alpha_{\mathrm{PA},i,k-1} I(f) \exp(-j2\pi f \tau) + N(f). \tag{20}$$

The estimated channel gain for the ith LED in the kth positioning trial is given by

$$\begin{aligned} \tilde{G}_{\mathrm{PA},i,k} &= \left\{ \frac{\mathbb{E}\left[|Y_{\mathrm{PA},i,k}(f)|^2\right]}{R^2 K^2 \alpha_{\mathrm{PA},i,k-1}^{2} \mathbb{E}\left[|I(f)|^2\right]} \right\}^{\frac{1}{2}} = \left\{ \frac{R^2 G_i^2 K^2 \alpha_{\mathrm{PA},i,k-1}^{2} \mathbb{E}\left[|I(f)|^2\right] + \mathbb{E}\left[|N(f)|^2\right]}{R^2 K^2 \alpha_{\mathrm{PA},i,k-1}^{2} \mathbb{E}\left[|I(f)|^2\right]} \right\}^{\frac{1}{2}} \\ &= \left\{ G_i^2 + \frac{\sigma_{\mathrm{N}}^2}{R^2 K^2 \mathbb{E}\left[|I(f)|^2\right]} \frac{\tilde{G}_{\mathrm{PA},i,k-1}^{2}}{3} \sum_{i=2}^{4} \frac{1}{\tilde{G}_{\mathrm{PA},i,k-1}^{2}} \right\}^{\frac{1}{2}}. \end{aligned} \tag{21}$$

The error of square of estimated transmission distance $\Delta D_{\mathrm{PA},i,k}^{2}$ using power allocation scheme for the ith LED in the kth positioning trial is given by,

$$\begin{aligned} \Delta D_{\mathrm{PA},i,k}^{2} &= \tilde{D}_{\mathrm{PA},i,k}^{2} - D_i^2 \\ &= \left\{ \frac{1}{D_i^{2(m+3)}} + \frac{\sigma_{\mathrm{N}}^2}{\left[\frac{RK(m+1)Ah^{m+1}}{2\pi}\right]^2 \mathbb{E}\left[|I(f)|^2\right]} \frac{\sum_{i=2}^{4} \tilde{D}_{\mathrm{PA},i,k-1}^{2(m+3)}}{3\tilde{D}_{\mathrm{PA},i,k-1}^{2(m+3)}} \right\}^{-\frac{1}{m+3}} - D_i^2. \end{aligned} \tag{22}$$

Optics EXPRESS

Note that $\tilde{D}^2_{\mathrm{PA},i,0}$ is the square of estimated distance ($\tilde{D}^2_i$) without using power allocation scheme, *i.e.*, $\tilde{D}^2_{\mathrm{PA},i,0} = \tilde{D}^2_i$. The power allocation stops, when the $\Delta D^2_{\mathrm{PA},i,k}$ is stable.

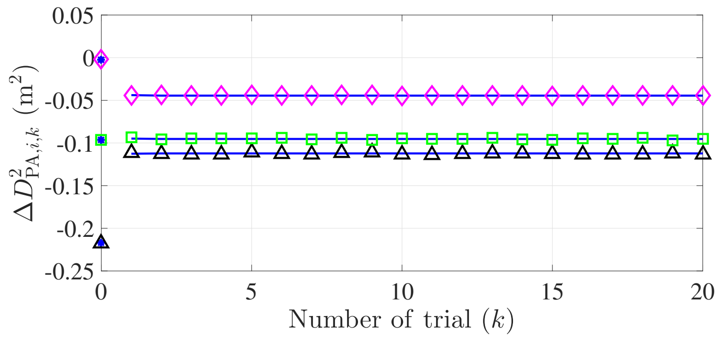

Fig. 11. $\Delta D^2_{\mathrm{PA},i,k}$ ($k \geq 1$) using power allocation scheme for the receiver at $[-4\ \mathrm{m}, -3\ \mathrm{m}, 1\ \mathrm{m}]^{\mathrm{T}}$. $k = 0$: without using power allocation scheme. Blue: theory, green: LED 2, pink: LED 3, black: LED 4.

Fig. 11 illustrates the performance of $\Delta D^2_{\mathrm{PA},i,k}$. The values of $\Delta D^2_{\mathrm{PA},i,k}$ ($i = 2, 3, 4$) converge after several power allocation trials. Hence, the power allocation is a fast algorithm. The converged values are -0.098 m^2, -0.043 m^2 and -0.11 m^2 for LED 2 to LED 4, respectively. Without using power allocation scheme, ΔD^2_i are -0.096 m^2, -0.0022 m^2 and -0.218 m^2 for LED 2 to LED 4, respectively, as shown in Fig. 12. Although the values of $\Delta D^2_{\mathrm{PA},i,k}$ are smaller than the minimum ΔD^2_i ($i = 3$), the differences among $\Delta D^2_{\mathrm{PA},i,k}$ are smaller than those of ΔD^2_i. The corresponding positioning errors are 0.011 m and 0.029 m when using and without using power allocation scheme, respectively, as shown in Fig. 13. Hence, the power allocation scheme is effective to reduce the positioning error further in determined VLP system using OFDMA.

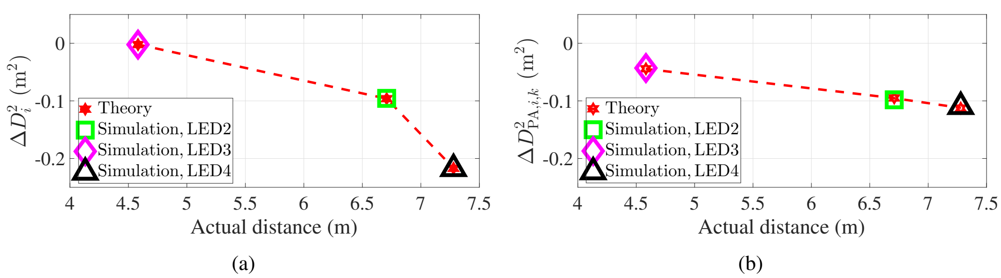

Fig. 12. $\Delta D^2_{\mathrm{PA},i,k}$ (a) without using and (b) using power allocation scheme.

Fig. 13 shows the positioning error in the whole room of determined VLP system using and without using power allocation schemes. The power allocation schemes reduces the positioning error, especially when the transmission distances are long. Without using power allocation scheme, the positioning errors are 0.049 m and 0.036 m, when the receiver locates at $[-4\ \mathrm{m}, -4\ \mathrm{m}, 1\ \mathrm{m}]^{\mathrm{T}}$ and $[-4\ \mathrm{m}, 0\ \mathrm{m}, 1\ \mathrm{m}]^{\mathrm{T}}$, respectively. Using the power allocation scheme, the corresponding positioning errors are reduced to 0.020 m and 0.0072 m for the two locations, respectively. The positioning accuracy are improved by 0.029 m (59%) and 0.029 m (81%), respectively. Therefore, the fast and effective power allocation scheme improves the positioning accuracy further in determined VLP system using OFDMA.

Optics EXPRESS

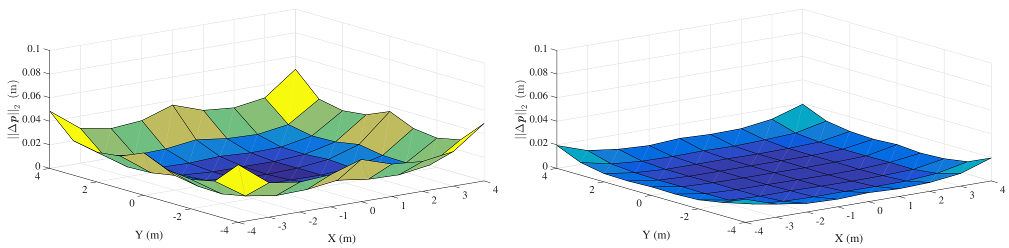

(a) (b)

Fig. 13. Positioning error of determined VLP system using OFDMA in the whole room: (a) without using power allocation scheme, (b) using power allocation scheme.

4. Conclusion

In this paper, we proposed a system that realized VLP and VLC simultaneously in the same band using OFDMA. We used the power of received data sequence in each subcarrier block as the metric for the estimation of transmission distance in terms of channel gain. Therefore, VLP did not deteriorate the performance of VLC. In this system, the differences among errors of square of estimated transmission distances are the critical factors in positioning error. We have investigated the following three method to reduce such differences and consequently to reduce the positioning error. In overdetermined VLP system, the positioning error fluctuates due to the redundant LED. To avoid such fluctuation, we selected the LED with the shortest transmission distance as the master LED. Then, we changed the overdetermined VLP system to determined VLP system by excluding one LED for positioning. This method reduced the positioning error, only when we excluded the LED with the longest transmission distance. The positioning error was reduced further in determined VLP system by using power allocation. The power was allocated to modulation signals according to the estimated channel gains on each subcarrier block. This method was fast and effective to improve the positioning performance. The matched theoretical and MC simulation results validated the proposed VLP based on VLC system using OFDMA.

Funding

National Natural Science Foundation of China (NSFC) (61601321, 61601247, 61271239).